PROXIMAL VOLCANIC DEPOSITS: ROUGHNESS AND IMPLICATIONS FOR LUNAR VOLCANISM.

J. D. Stopar [1], S. J. Lawrence[1], M. S. Robinson[1], L. R. Gaddis[2], T. A. Giguere[3], S. Sutton[4], and the LROC Team, [1]SESE, Arizona State University, Tempe, AZ, [2]USGS Flagstaff, AZ, [3]HIGP, University of Hawaii, Honolulu, HI, [4]LPL, University of Arizona, Tucson, AZ.

Introduction: A variety of localized, positive-relief topographic features (<10-100 km^2 in extent) on the Moon are interpreted as volcanic [e.g., 1-12] (**Fig. 1**), including cones, lava flows, dark hills, and pyroclastic deposits. Small-area deposits observed with LROC NAC imaging occur proximal to their source vent and provide new insights into the range, volatility, and timing of lunar volcanism.

Landforms: *Small cones:* Small volcanic cones (< 3.5 km in diameter and steep-sided [1-3]) with conical to elongate summit craters occur in most nearside mare [1-8,10-11]. Summit-diameter to base-diameter relationships of the small cones (0.04-0.1) are distinct from those of classic domes and pyroclastic (localized dark mantling deposits - DMD) vents [2]; cone vent widths are relatively large compared to the base diameter. Criteria for identifying cones [1] should be applied only in consideration of geologic context. For example, many impact craters, or features of uncertain origin, have similar morphologies, but are unlikely to be volcanic vents due to their occurrence in chaotic impact debris.

Small cones are interpreted to be constructed from cinder and spatter, with a large contribution from lava flow remnants contributing to the proximal vent morphology (based on rille-like channels, and C-shapes) [1]. Flank slopes range from 10° to >20°, but are gentler than most fresh terrestrial cinder cones (~30°) [3]. Lunar flank slopes are expected to be lower as a result of decreased gravity [5]. Flank slopes also reflect physical properties (e.g., the relative abundances of pyroclastics, spatter, and lava) [1] and are likely lower when lava flows, and less cinder/spatter, are present.

Intermediate cones: Two cones in Mare Crisium are larger in diameter (3.5 and 6.0 km, respectively) than the small cones, but have lower height/base diameter ratios ~0.02-0.03 and flank slopes (~8°) [3]. Both Crisium cones have breached summit craters and are distinct in morphology from typical lunar domes [2]. Both have summit craters at or just below the elevation of the surrounding mare. They are superficially similar in morphology to tuff cones on both Earth and Mars [13], with a relatively wide crater. However, the Crisium cones are embayed by younger lava flows, and the original base cone morphology may be obscured.

Irregular clusters of vents and flows: "Dark hills" are low-reflectance, irregular mounds that occur in volcanic terrain, are lower reflectance than surrounding mare, and may represent proximal lava flows or spatter that did not form a distinctive cone structure. "Domes" or low shields in the Marius Hills, exhibit stratigraphic relationships that suggest a shield construction process through a sequence of localized lava eruptions and cone-building events [e.g., 14].

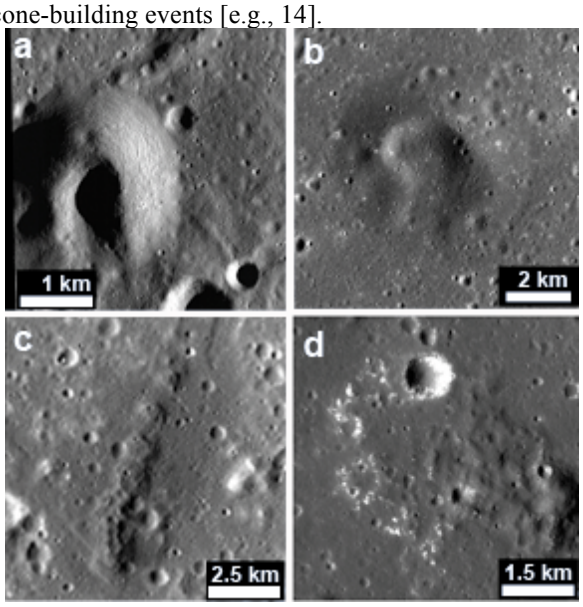

Fig. 1. *LROC NAC images of small volcanic vents and cones: a) small C-cone (Marius Hills); b) intermediate cone (Crisium); c) aligned or linear vents and deposits (Rima Parry); d) rough, blocky lava flow and cone (Marius Hills [1]).*

NAC-derived Roughness: We calculated NAC-based slopes and roughnesses for several volcanic landforms using NAC digital terrain models (DTMs; **Fig. 2**). These results are complementary to those of previous radar investigations [1,15]. The NAC-derived roughness is expressed as TRI (terrain ruggedness index [16]), the average elevation difference between pixels in a 3x3 grid and the central pixel (pixel scale 10 m). Ponded melt deposits are the smoothest landforms on the Moon at the 10-m scale (slopes=<2°, 10-m TRI<0.22m). Mare have greater slopes (2-4°) and TRIs (0.22-0.5m), and are similar to those of localized DMDs, suggesting the mantling deposits are relatively thin. Small-area flows found proximal to some cones and dark hills exhibit steeper slopes (6-8°) and greater TRIs (0.65-0.9m) than mare. Highlands materials have even greater slopes (8-12°) and TRIs at the 10-m scale (>1.0m) and are distinct from the volcanic terrains.

Implications for Lunar Mare Volcanism: The timing of lunar cone formation and other small area deposits is difficult to constrain, as areas and slopes are not favorable to standard crater counting techniques. If

we assume that cones formed contemporaneously with nearby mare flows, they are roughly Imbrian-Eratosthenian in age, corresponding to the timing of the most mare volcanism [e.g., 17-18].

An end-member model of mare volcanism describes large expanses of mare as being deposited from several large vents [e.g., 19-20]. Other models stress that mare volcanism involves numerous eruptions from scattered smaller vents [e.g., 21-22]. The wide distribution of cones, and other volcanic vents, supports the hypothesis of mare volcanism from a large number of widely dispersed sources, including more frequent and numerous smaller eruptions than is generally considered. Alternatively, some proximal deposits may be rootless eruptions. However, regional concentrations like those of the Marius Hills, which exhibit evidence of repeated eruptions, could potentially derive from a single source [14,23-24]. Small cones and associated lava flows may, therefore, represent eruption of residual, late-stage materials, as the source magma evolved over time [e.g., 4,8,20,25].

The distribution of small cones corresponds to a wide range of regional LP Th abundances (**Fig. 3**), and most cones are located in regions of >3.5 ppm Th (the cutoff of the PKT [26]), and thus, could be a component of long-lived volcanic activity. However, the sampling scale of the Th data (0.5°) is much greater than the diameter of the cones (0.5-3 km), and this association is speculative.

Assuming little magma evolution, cones formed from the same source regions as maria will have similar pre-eruptive volatile contents (though perhaps different ascent rates). Given recent models calling for a range in source-region volatile contents for the lunar glasses and mare basalts [e.g., 27-29], heterogeneous distributions of magma volatiles may help explain the various observed cone (and DMD) morphologies.

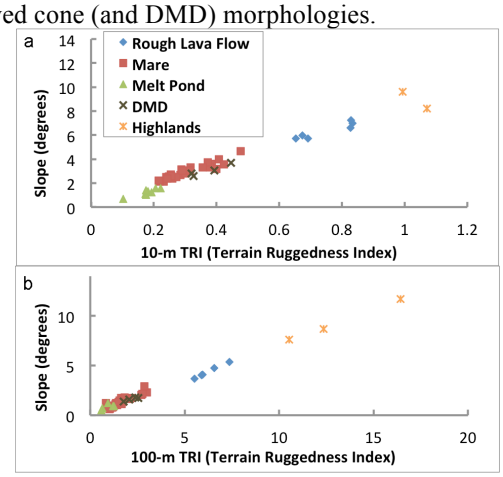

Fig. 2. *Slopes and roughnesses (as TRI) of different types of landforms derived from a) 10-m slope and elevation data and b) 100-m data.*

Summary: Our preferred model of cone formation is one in which the cones are a by-product of mare eruptions from multiple sources, although the cones of the Marius Hills may be related to shield volcanism. Layering in small C-cones indicates variable or intermittent explosive eruptions, likely related to comparatively slow ascent rates [e.g., 2, 8, 30]. The C-cones in the Marius Hills tend to be larger and steeper than those found elsewhere [3], and may be a consequence of increased volatiles and/or larger eruption volumes. Lava flows associated with small cones represent volatile-depleted eruptions [e.g., 8], and are rougher than mare flows. Moderately explosive origins are suggested for the intermediate-sized cones, but these eruptions are less explosive than the eruptions forming the localized DMDs.

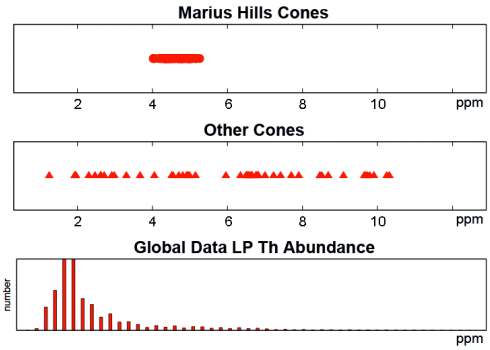

Fig. 3. *LP Th values (ppm) for areas including cones.*

References: [1] Lawrence, et al. (2013) *JGR* 10.1002/jgre.20060. [2] Stopar, et al. (2015) *LPSC* # 1474. [3] Stopar, et al. (2014) *LPSC* #1425. [4] McCauley (1967) USGS Map I-491. [5] McGetchin and Head (1973) *Sci.* 180: 68-71. [6] Schaber (1973) *Apollo 17 Prelim. Sci. Rep.* p.30-17—30-25. [7] Scott and Eggleton (1973) *USGS Map I-805*. [8] Weitz and Head (1999) *JGR* 104: 18933-18956. [9] Sruthi and Senthil Kumar (2014) *Icarus*, 249-268. [10] Schultz (1976) *Moon Morph*., 604 pp. [11] Masursky, et al. (1978) *NASA SP-362*. [12] Head and Wilson (1979) *Proc. 10th LPSC*, 2861-2897. [13] Brož and Hauber (2013) *JGR*, 10.1002/jgre.20120. [14] Spudis et al. (2013) *JGR*, 10.1002/jgre.20059. [15] Campbell et al. (2009) *JGR*, 10.1029/2008JE003253. [16] Wilson et al. (2007) *Mar. Geod.* 30, 3-35. [17] Wilhelms and McCauley (1971) *USGS Map I-703*. [18] Hiesinger et al. (2011) *GSA Paper 477*, 1-51. [19] Greeley (1971) *Moon* 3, 289-314. [20] Whitford-Stark and Head (1977) *Proc. LPSC*, 2705-2724. [21] Wilhelms (1987) *USGS Paper 1348*. [22] Hörz et al. (1991) *Lunar Sourcebook*, ch. 4. [23] Wilson and Head 2001 *LPSC* #1297. [24] Kiefer (2013) *JGR*, 10.1029/2012JE004111. [25] Heather et al. (2003) *JGR* doi:10.1029/2002JE001938. [26] Jolliff et al. (2000) *JGR* 105, 4197-4216. [27] McCubbin et al. (2011) *GCA* 75, 5073-5093. [28] Robinson and Taylor (2014) *Nat. Geo.*, 10.1038/ngeo2173. [29] Hauri et al. (2015) *EPSL* 409, 252-264. [30] Wilson and Head (1981) *JGR* 86, 2971-3001.